Journal of Sound and Vibration 329 (2010) 4810–4828

Contents lists available at ScienceDirect

Journal of Sound and Vibration

journal homepage: www.elsevier.com/locate/jsvi

Aeroacoustics research in Europe: The CEAS-ASC report on 2009 highlights

Damiano Casalino

CIRA, Italian Aerospace Research Center, via Maiorise, 81043 Capua, Italy

A B S T R A C T

The Council of European Aerospace Societies (CEAS) Aeroacoustics Specialists Committee (ASC) supports and promotes the interests of the scientific and industrial aeroacoustics community on an European scale and European aeronautics activities internationally. In this context, "aeroacoustics" encompasses all aerospace acoustics and related areas. Each year the committee highlights some of the research and development projects in Europe.

This paper is a report on highlights of aeroacoustics research in Europe in 2009, compiled from information provided to the ASC of the CEAS.

In April 2009, the Level-2 project OPENAIR of the Seventh Framework Programme of the European Commission has been launched with the goal of delivering a step change in noise reduction, beyond the successful achievements of the predecessor SILENCE(R).

Some contributions submitted to the editor summarizes findings from programmes launched before 2009, while other contributions report on activities supported by national associations and industries. Furthermore, a concise summary of the workshop on "Resolving Uncertainties in Airframe Noise Testing and CAA Code Validation" held in Bucharest is included in this report. Enquiries concerning all contributions should be addressed to the authors who are given at the end of each subsection.

1. CEAS-ASC workshop

The workshop on "Resolving Uncertainties in Airframe Noise Testing and CAA Code Validation" was held on 1–2 October 2009 at the The Palace of Parliament in Bucharest, Romania. It was the 13th workshop sponsored by the ASC of CEAS, the third one to be sponsored by the Aeroacoustics Committee of AIAA, and the fourth one to be financially supported by the X3-Noise collaborative network project of the European Commission. The workshop was locally organized by Sorin Gabroveanu, from the National Research and Development Institute for Gas Turbines (COMOTI). The chairman of the scientific committee was Lars Koop from DLR (German Aerospace Center), who will act as guest editor of a special issue of the International Journal of Aeroacoustics dedicated to the workshop. The subject of "Airframe Noise Testing and CAA Code Validation" has gained increasing interest recently, as computational aeroacoustics becomes more and more important within the future quiet aircraft design process to achieve the reduction of noise emission by aircraft postulated in the ACARE VISION 2020 agenda. The workshop started with a keynote lecture given by David Lockard from NASA Langley about "CAA validation and benchmark experiments for airframe noise: needs, challenges and near term prospects" in which the general issue of data accuracy obtained from both numerical calculations and validation experiments was addressed. The benefit to be expected from particle image velocimetry experiments in the field of

E-mail address: d.casalino@cira.it

0022-460X/$ - see front matter © 2010 Elsevier Ltd. All rights reserved.
doi:10.1016/j.jsv.2010.06.001

airframe noise have been discussed by Klaus Ehrenfried from DLR in his keynote lecture about the "Application of particle image velocimetry in aeroacoustics". Eric Manoha from ONERA presented in a third keynote lecture the activities in the LAGOON project which is dedicated to a large scale validation experiment on a landing gear measurement setup: "LAGOON: an experimental database for the validation of landing gear noise prediction methods". The 15 papers presented to 51 participants were divided into four sessions in which "scaling and Reynolds number effects", "recent developments in CAA and code validation", "numerical methods for wind tunnel correction" and "advances in aeroacoustic testing" have been addressed. The meeting was closed by a panel discussion where the main topics and prospects resulting from the presentations and key issues for the next years also with regard to the translational benchmark experiments have been discussed.

Written by L. Koop: Lark.Koop@dlr.de, DLR, Germany.

2. European-funded projects: OPENAIR

As part of the 7th Framework Programme, OPENAIR (OPtimisation for low Environmental Noise impact AIRcraft) started on 1st April 2009 as a four-year program with a total budget of 30 million euros financed with 18M by the European Commission. Snecma (SAFRAN Group) is the coordinator, leading a consortium of 47 partners including European major aerospace industries (Airbus, Aircelle, Bombardier, Dassault Aviation, EADS, GKN Aerospace, ITP, Messier-Dowty, Rolls-Royce, Snecma Propulsion Solide, Volvo), research institutes and small businesses.

OPENAIR aims to deliver a 2.5 dB source noise reduction, beyond the SILENCE(R) achievements. The program will focus on the validation of new technologies, such as introduction of electronically assisted solutions, the application of improved computational aeroacoustics, new affordable absorbing materials and airframe noise solutions. It will also include the identification of applicability over the product range, as well as the analysis of benefits for different market segments. OPENAIR's multidisciplinary approach and composition is suited to the projected integrated, lightweight solutions.

By adopting an integrated aircraft approach based on the latest developments in active and adaptive technologies, flow control techniques and advances in computational aeroacoustics applied in all areas, OPENAIR will deliver the breakthrough that is needed to achieve the 2020 ACARE goals.

Written by E. Kors: eugene.kors@snecma.fr, Snecma, France.

3. Airframe noise

3.1. Prediction of gap and overlap effect on slat noise and experimental validation

In the framework of the EU project TIMPAN, broadband sound generation from a three-element high-lift configuration were simulated with a hybrid RANS/CAA method and validated against experiments conducted in the acoustic wind tunnel of DLR (AWB). The aeroacoustic simulations are carried out with the DLR CAA code PIANO. The effect of slat gap and overlap on sound generation was studied. The slat gap is the smallest distance measured from the slat trailing edge to the main element surface, whereas the overlap is defined as the distance from the slat trailing edge to the nose of the main element, measured in a direction parallel to the clean chord, as illustrated in Fig. 1(a). In the simulation approach the RPM method [1] is used as a 4D synthetic turbulence generator to translate the steady one-point statistics and turbulent length- and time-scales of RANS into fluctuations of turbulent velocity. The whole approach represents a methodology to solve statistical noise theories with state-of-the-art CAA tools in the time-domain. Due to its efficiency compared to highly resolved unsteady CFD simulation, a greater number of configurations can be studied. In total 43 individual slat-gap and overlap combinations were simulated within TIMPAN. CAA simulations were performed for all matrix positions, making

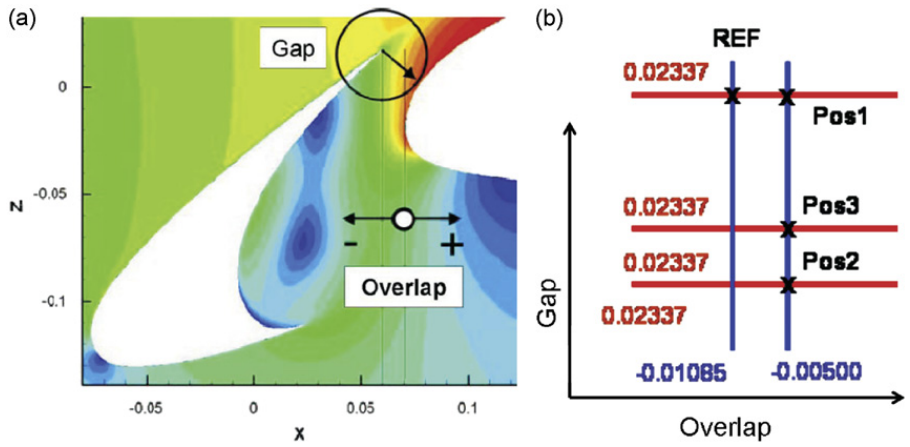

Fig. 1. RANS-RPM prediction of slat noise. (a) Definition of setting parameters, (b) investigated slat settings.

use of a set of RANS computations provided by Airbus. The CAA computations were conducted as a blind prediction in advance of the measurements conducted in the AWB. From this setting matrix four slat settings were selected, as sketched in Fig. 1(b), for which narrow band and one-third octave spectra from RANS were compared with measurements. Good agreement of the noise trends could be found between CAA and experiments. Especially, the specific shape of the spectra could be realised with CAA over the numerically resolved frequency bandwidth. The difference in level between the selected configurations was obtained qualitatively and quantitatively by CAA. More important, the peculiar characteristics of these different settings could be predicted based on just one single calibration of the model parameters. Fig. 2 presents a comparison of narrow-band spectra from experiment and simulation. The characteristic roll-off of the spectra is captured. A noise reduction potential of up to 8 dB was found between Position 1 (gap open) and Position 2 (small gap) in the experiment and the simulation. The levels of the intermediate gap setting Position 3 lies between these two settings, similar well resolved by experiment and simulation.

Written by R. Ewert: roland.ewert@dlr.de, DLR, Germany.

3.2. Two-step simulation of slat noise

Airframe noise has a pronounced impact on urban residents in the vicinity of metropolitan airports where the number and capacity of aircraft transport increase annually. In the literature, the noise generation mechanisms of high-lift devices, landing gears, and fuselage have been investigated to develop a low-noise design at low-fuel consumption. In the recent numerical study König et al. [2] show the main vortex sound source to be the shear layer, which emanates from the slat cusp and impinges upon the lower slat surface. Furthermore, the cross-correlation analysis identifies the fluid-acoustics mechanism where the strong pressure pulsation is triggered by spatial fluctuations of the impinging shear layer. These findings show active control via manipulation of turbulent structures [3] to be a reasonable method to suppress the strong noise generated near the slat (Fig. 3).

Written by D. König; s.koh@aia.rwth-aachen.de, S. R. Koh, M. Meinke and W. Schröder, Institute of Aerodynamics of the RWTH Aachen University, Germany.

3.3. Broadband trailing edge noise prediction with a stochastic source model

Airfoil self-noise is one of the most important components of the broadband noise emitted by lifting surfaces. In Ref. [4] a computational technique for the numerical simulation of the self-noise radiated by a wing profile has been developed. The evaluation of the turbulent noise sources responsible for acoustic radiation is obtained by an Eulerian solenoidal digital filter (ESDF) method. The reconstruction of the fluctuating turbulent velocity components is obtained from the time-averaged turbulence quantities, solution of the steady-state RANS equations, by a stochastic reconstruction approach. The validation with a classical test-case, the homogeneous and isotropic turbulence in a two-dimensional square, shows that the ESDF method is able to correctly reproduce the space–time turbulence statistics. The near-field acoustic radiation is computed solving the acoustic perturbation equations in the frequency domain with a finite element discretization. Far-field directivities are evaluated with the Ffowcs-Williams & Hawkings integral formulation. Numerical results for the broadband trailing edge noise radiated by a NACA-0012 profile have been compared with experimental results available in

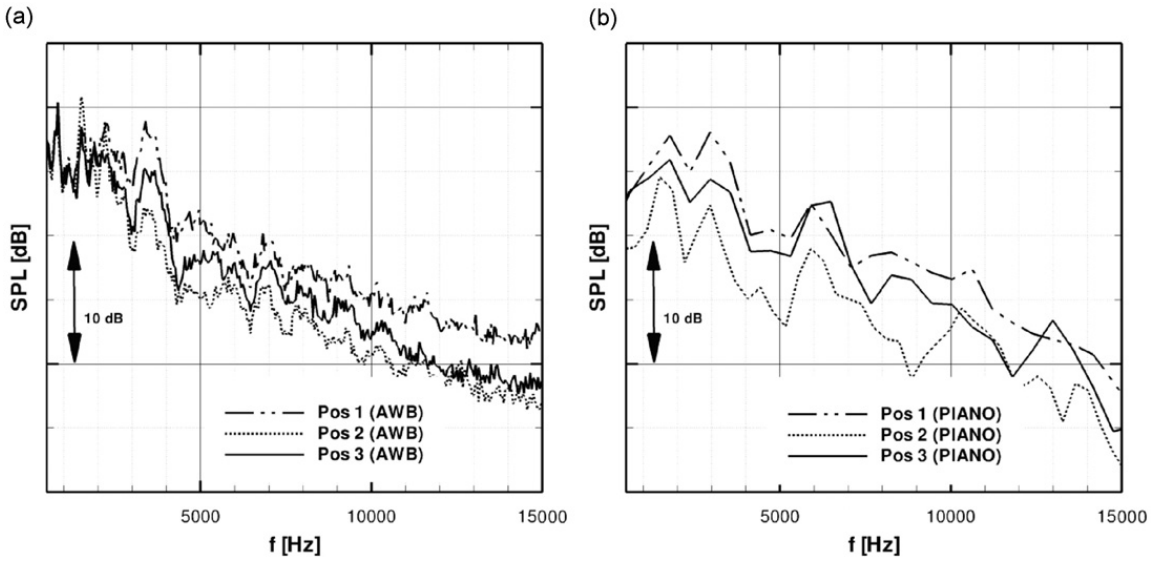

Fig. 2. Comparison measurements and prediction: narrow-band spectra. (a) Measurements—AWB, (b) prediction—PIANO.

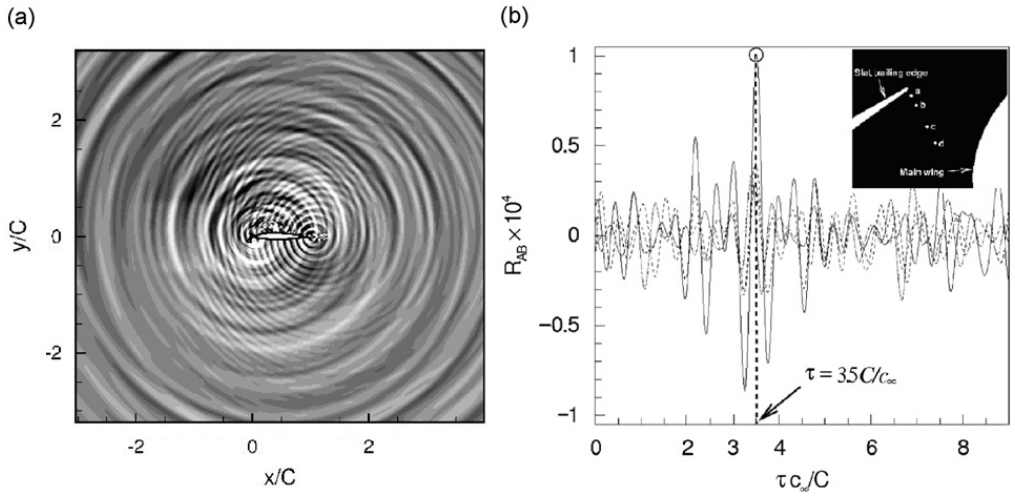

Fig. 3. Acoustic field determined by the acoustic perturbation equations, (a) instantaneous acoustic pressure contours, (b) cross-correlation of acoustic pressure and near-field noise source.

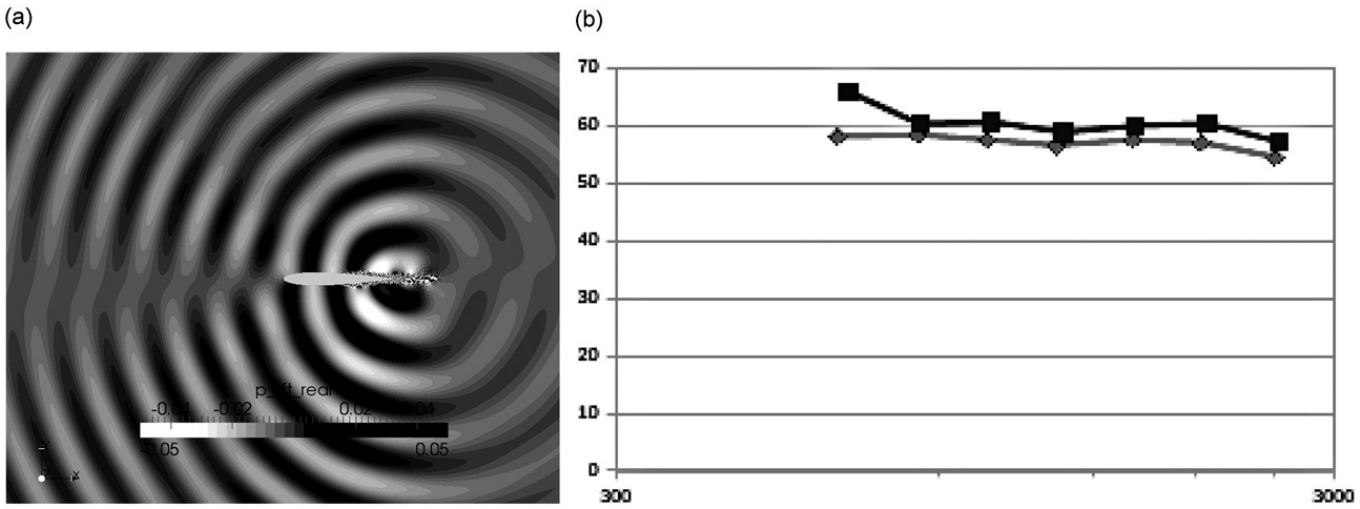

Fig. 4. RANS-ESDF prediction of airfoil trailing edge noise: Re=1.16×10^6, M=0.162, $\alpha = 0$. On the left: ■ numerical results, ♦ experimental results (Brooks et al. [5], airfoil self-noise and prediction, NASA T.R., Reference publication 1218, 1989). (a) Near-field instantaneous acoustic pressure (f=2344 Hz), (b) far-field acoustic pressure power spectral density (r=1.22 m, $\theta = 90^\circ$).

literature. In Fig. 4(a) an example of near-field radiation is shown. In Fig. 4(b), the 1/3 octave acoustic pressure power spectral density at far-field point is shown and compared with literature experimental results.

Written by R. Arina: renzo.arina@polito.it, I. Cozza and A. Iob, Politecnico di Torino, Italy.

3.4. Prediction of wind turbine noise and validation against experiment

A semi-analytical, semi-empirical prediction method for trailing edge noise was successfully applied to calculate the noise from two modern large wind turbines [6]. Based on only blade geometry and turbine operating conditions (RPM, wind speed and blade pitch angle), good agreement was found between measurements and predictions for (i) the noise source distribution in the rotor plane as a function of frequency and observer position, (ii) the turbine noise directivity and the variation in sound level during the revolution of the blades (swish), and (iii) the source spectra and overall sound levels. The difference between predicted and measured levels for a range of wind speeds was less than 1–2 dB, as shown in Fig. 5. The validated code was then applied to calculate the time-dependent noise footprints, which showed that for cross-wind directions the average level is lower than for up- and downwind directions, but the level variation is larger.

Written by S. Oerlemans: stefan@nlr.nl, National Aerospace Laboratory NLR, The Netherlands.

4. Fan and jet noise

4.1. Direct noise computation and investigation of sound sources for a coaxial heated jet

A coaxial jet originating from coplanar pipe nozzles has been computed by compressible large eddy simulation (LES) using low-dissipation and low-dispersion numerical schemes, to determine its acoustic field and to study noise generation mechanisms [7]. The jet streams are at high velocities, the primary stream is heated, and the Reynolds number based on the primary velocity U_p and the secondary diameter D_s is around 10^6. High levels of turbulent intensities are also specified at the nozzle exit. The jet flow and near-pressure fields are both obtained directly from the LES. A snapshot of the pressure field is shown in Fig. 6(a). The far-field noise is calculated by solving the linear acoustic equations, from the LES data on a cylindrical surface. A good agreement is observed in terms of sound pressure directivity, levels and narrow-band spectra with measurements obtained during the EU project CoJeN for a jet with similar initial conditions. A comparison between measured and predicted acoustic spectra is shown in Fig. 6(b). High correlations are in addition found between the pressure radiated in the downstream direction, and turbulent quantities around the end of the primary and secondary potential cores, indicating that noise generation is significant in these flow regions as in single jets [8].

Written by C. Bogey: christophe.bogey@ec-lyon.fr, Ecole Centrale de Lyon, France.

4.2. 3D numerical simulations of the aft fan noise emitted by a realistic turbofan engine

Fan noise is a major harmful aircraft sound source, especially during take-off and approach flight phases. For a long time, motorists and manufacturers mainly investigated the prediction/reduction of fan noises' upstream component

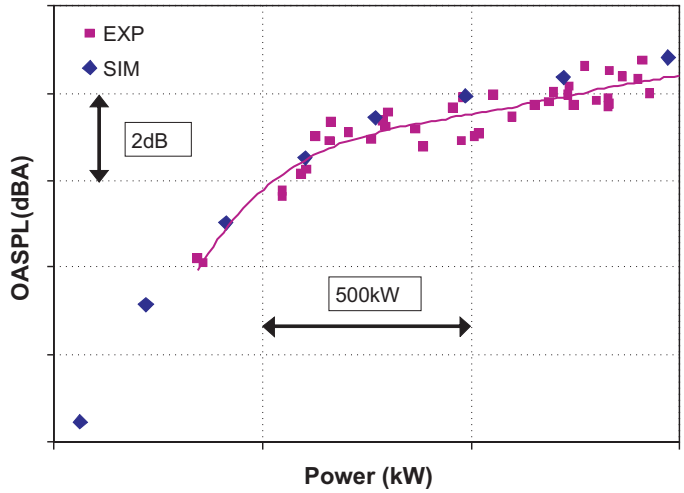

Fig. 5. Measured (■) and predicted (♦) turbine noise level as a function of rotor power.

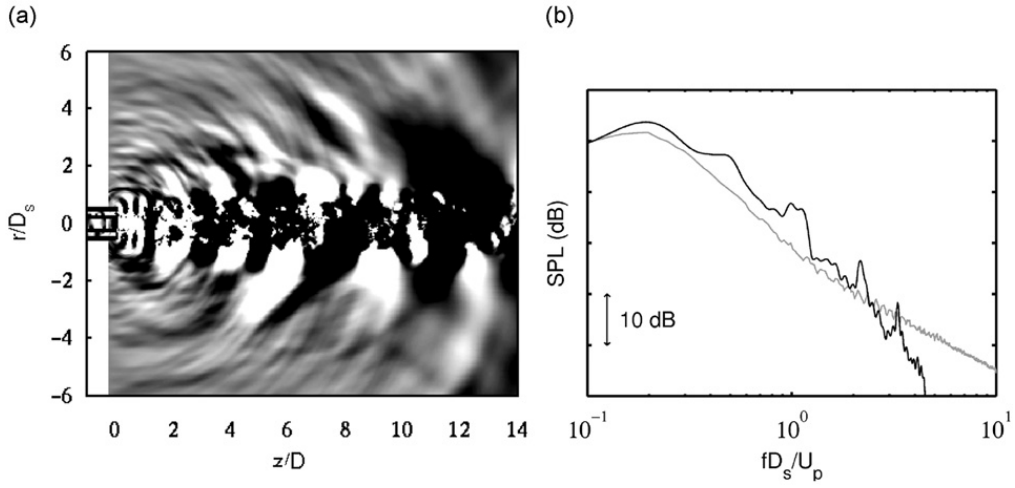

Fig. 6. Coaxial heated jet noise prediction. (a) Snapshot of fluctuating pressure obtained directly by LES. The gray scale is defined for variations between −130 and 130 Pa, (b) far-field pressure spectra from the simulation (black) and from CoJeN experiment (gray), for an emission angle of 30°, as functions of Strouhal number fD_s/U_p.

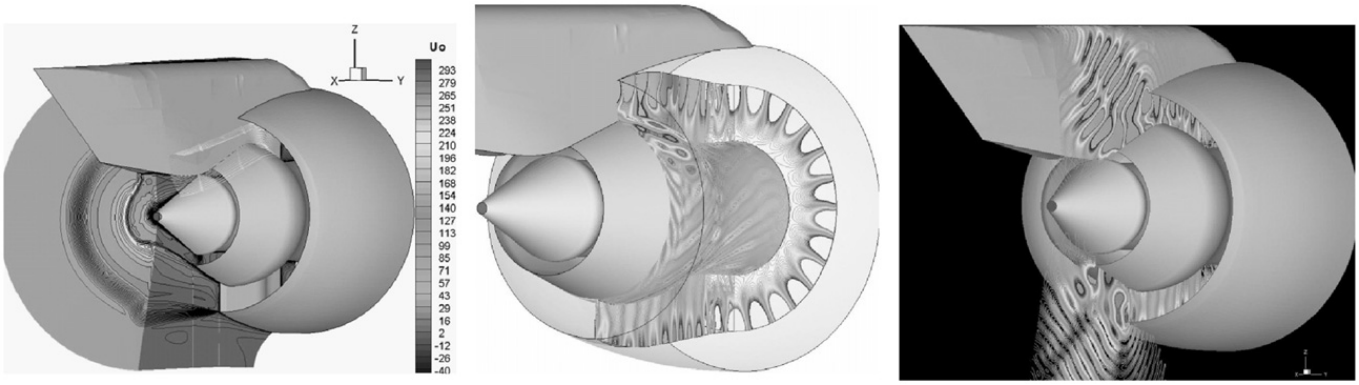

Fig. 7. Acoustic radiation of an aft fan noise $(m,n)=(13,1)$ emitted at the blade-passage frequency by a realistic exhaust in take-off conditions: mean flow (x-velocity, left), instantaneous perturbed pressure fields internally propagated (middle) and externally radiated (right).

(which is emitted by the engine's air intake). Since a few years, they also focus on the more complex problem of predicting/reducing its downstream component (which is emitted through the exhaust, and its highly inhomogeneous jet flow). Within such framework, a collaborative Airbus/ONERA study has been recently conducted [9,10], which consisted in CAA-characterizing the aft fan noise emissions of a realistic full-3D exhaust ('realistic' meaning here 'with pylon and internal bifurcations'). Such engine was allotted with (i) representative thermodynamic conditions and/or (ii) relevant fan noise modal contents, both being dictated by the industrial constraints. At the end, several inter-dependent calculations were conducted on the basis of the same "full-3D exhaust aft fan noise" configuration, each calculation differing from the others by both (i) the azimuthal order of the fan noise mode to be emitted, and/or (ii) the thermodynamic conditions to be accounted for. The computations were achieved using the sAbrinA.v0 solver [11,12], a classical CAA code developed at ONERA. Highlighting the installation effects to which acoustic waves are submitted to, when propagating inside and outside an exhaust, these results shown how far the full-3D nature of a turbojet engine can strongly affect its noise emission. Such conclusion is of importance since it indirectly demonstrates the crude necessity of accounting for the engines' inter/outer devices when estimating the noise radiation emitted by an exhaust. As an illustration, Fig. 7 shows the acoustic field radiated by the exhaust at take-off, when emitting an aft fan noise mode of azimuthal/radial orders (13,1) at the blade passing frequency.

Written by S. Redonnet: stephane.redonnet@onera.fr, C. Mincu and E. Manoha, ONERA, France.

4.3. A frequency-domain linearized Euler model for turbomachinery noise radiation through engine exhaust

Noise radiation through engine exhausts is an important issue for the aero-engine design. In the frame of a collaboration with AVIO, a numerical model for the exhaust noise radiation problem has been developed [13,14]. In the model it is assumed that an incoming wave is propagating through the exhaust nozzle, or the fan duct, and radiating outside. The near-field propagation is based on the solution of the linearized Euler equations in the frequency domain: for each wavenumber, a linearized Euler problem is solved using a finite element method on unstructured grids for arbitrarily shaped axi-symmetric geometries. The frequency-domain approach enables the suppression of the Kelvin–Helmholtz instability waves, moreover each single calculation, limited to a single frequency, is well suited to the exhaust noise radiation problem where the incoming wave can be treated as a superposition of elementary duct modes. To reduce the memory requirements, a stabilized continuous Galerkin formulation with linear triangular and quadrangular elements is employed and the global matrix inversion is performed with a direct solver based on a parallel memory distributed multifrontal algorithm for sparse matrices [15]. The acoustic near field is then radiated in the far field using the formulation of Ffowcs-Williams and Hawkings. The Munt problem has been calculated in order to validate the numerical model. Two turbomachinery configurations, defined in the frame of the project TURNEX, have been compared with numerical solutions and experimental data. In Fig. 8 an SPL directivity for the 'long cowl nozzle" configuration has been compared with TURNEX experimental data and the numerical results.

Written by R. Arina: renzo.arina@polito.it and A. Iob, Politecnico di Torino, C. Schipani, AVIO, Italy.

5. Techniques and methods in aeroacoustics

5.1. Experimental evidence of hydrodynamic instability over a liner in a duct with flow

The combined effect of wall property and vortex sheet is very often described by the Myers boundary condition. Recently, it has become clear that this limit leads to an ill-posed problem [16] and that a thin boundary layer flow along a lined wall may be unstable [17]. An experimental study with PIV and LDV [18] shows the presence of this instability and allows the measurements of the flow perturbations. From this experiment, the wavelength, the convection speed and the

growth of the instable hydrodynamic wave can be determined (see Fig. 9). One striking point is that the mean flow ($M \simeq 0.3$) in the experiment can be substantially modified by the presence of an acoustical wave.

Written by Y. Aurégan: yves.auregan@univ-lemans.fr and D. Marx, LAUM, France.

5.2. An indirect technique to globally characterize locally reacting liner

To achieve environmentally acceptable commercial aircraft to develop highly acoustic efficient duct treatments is still critical. A continuing concern in treatment technology is the determination of the impedance of an acoustic material in real conditions. Many conventional and innovative test liner structures generate complex acoustic fields specially with flow, scattering energy into higher order modes. This complicating feature cannot be handled by the traditional unidirectional, single mode propagation model method. Therefore, in the University of Technology of Compiegne, a technique to measure the homogenized impedance of a locally reacting liner mounted on the wall of a cylindrical barrel has been carried out, beginning in the no flow case, but assuming higher order modes acoustic propagation conditions. The homogenized acoustic normalized impedance of a liner placed on the wall of a barrel is educed by minimizing a cost function defined by the difference between the numerical and the experimental multimodal acoustic power dissipations of the barrel [19]. The dissipations are deduced from the numerical calculation and measurement [20] of the barrel multimodal scattering matrices. A good agreement is found when the experimental dissipation of the actual barrel is reduced by the experimental dissipation of a reference barrel where the liner was removed leaving only the barrel skin. Indeed, in Fig. 10(a) the educed normalized acoustic impedance results are found to be closed to results calculated with Elnady's semi-empirical model. Also, two scattering matrix coefficients of the barrel (the plane wave transmission and (1,0) mode reflection) numerically recalculated using the educed impedance are compared with those calculated with the Elnady's impedance pointing out a good agreement, as shown in Fig. 10(b).

Written by M. Taktak: jean-michel.ville@utc.fr, UTC, France.

5.3. A methodology for identifying the unsteady flow field responsible for the absorption of acoustic energy by orifices

This work considers the mechanism by which acoustic energy is absorbed by circular holes and other orifices by the generation of an unsteady flow field that cannot be converted back into acoustic energy. Flow visualization of such an unsteady flow field associated with nonlinear absorption is shown in Fig. 11 which, in this case, is dominated by vortex rings. Whilst

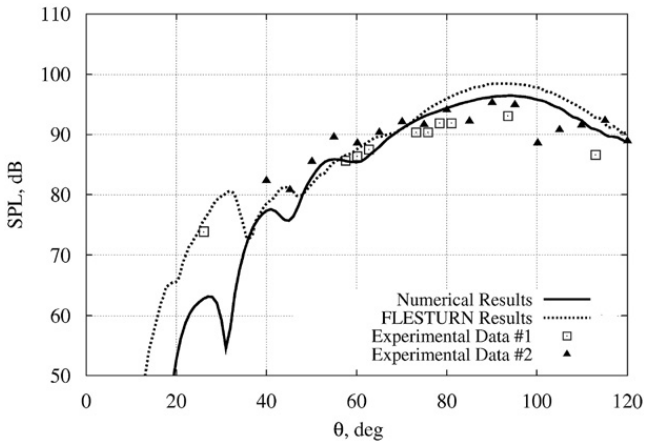

Fig. 8. Long Cowl Nozzle, static-cutback condition, modes (9,1-2), f=5742.5 Hz. Far-field solution, SPL directivity: comparison between superposition of numerical modes and experimental results.

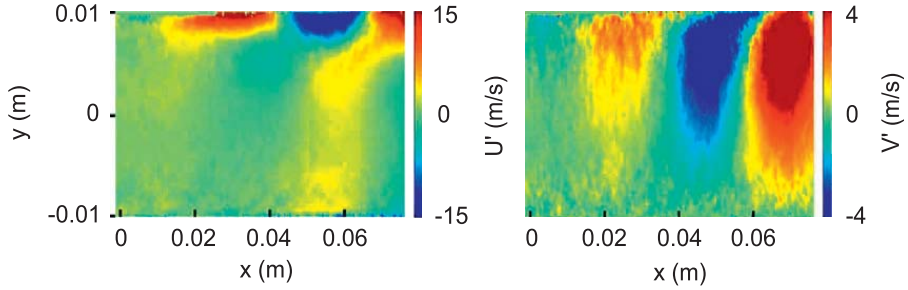

Fig. 9. PIV maps of the phase-averaged axial (U' on the left) and transverse (V' on the right) velocities in the channel, with the lined wall on the top.

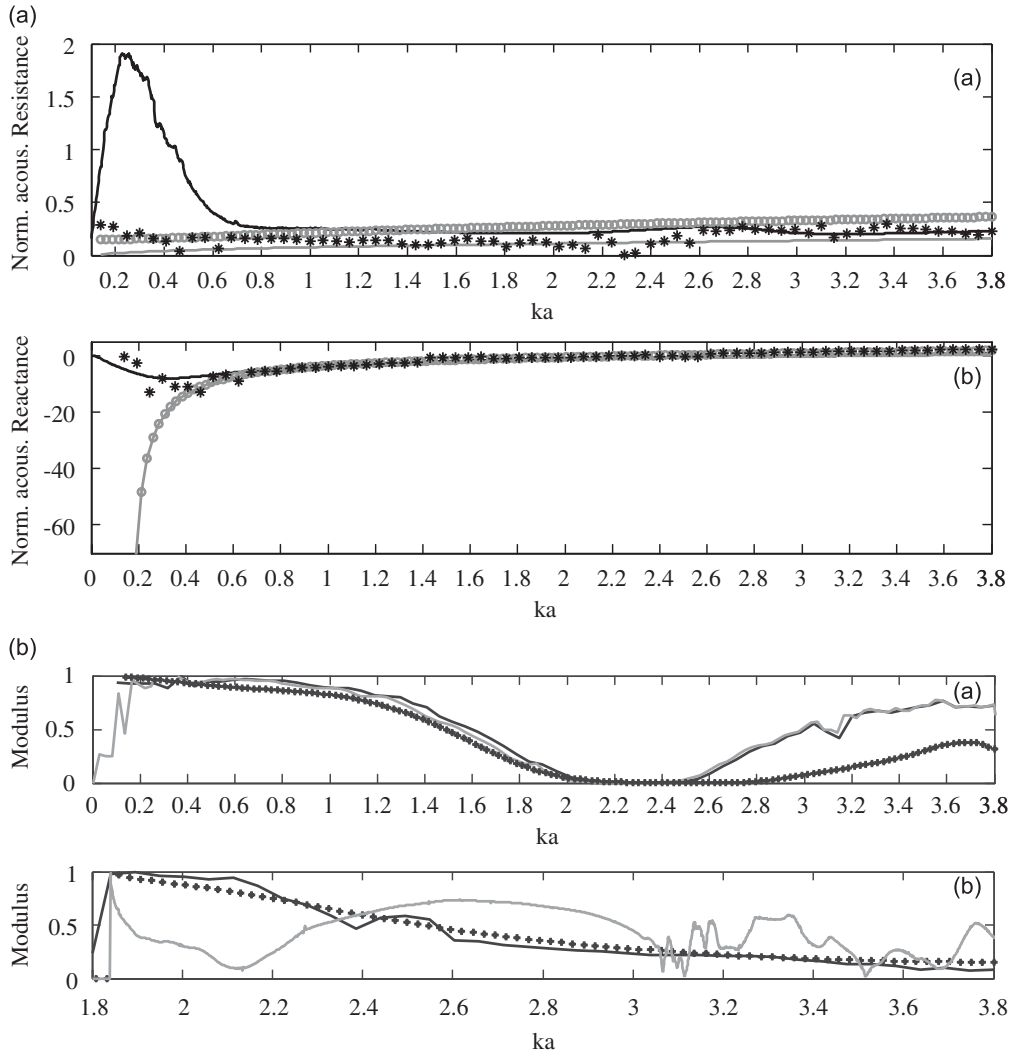

Fig. 10. Liner properties: educed (⋆), Elnady (•), Guess (light line) and TMM (dark line). (a) Normalized acoustic resistance (top) and reactance (bottom), (b) scattering matrix coefficients: $S^{21}_{00,00}$ (top) and $S^{11}_{-10,-10}$ (bottom).

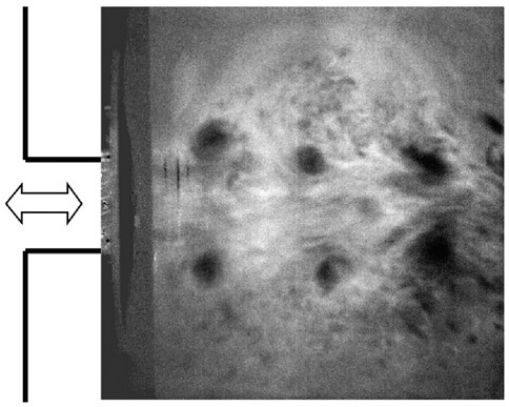

Fig. 11. Flow visualization of an example velocity field associated with nonlinear absorption.

common to a variety of engineering applications particular emphasis in this work has been placed on obtaining enhanced damping for aero gas turbine combustion systems. Experimental results have been obtained for a single orifice exposed to plane acoustic waves within a rectangular duct. Measurements of unsteady pressure enable the acoustic power absorbed by the orifice to be determined, whilst particle image velocimetry (PIV) is used to measure the unsteady flow field. By proper orthogonal decomposition (POD) analysis [21] the unsteady flow field can be decomposed into a number of modes and, via examination of each modes temporal coefficient, the modes associated with the incident acoustic pressure field can be

identified [22]. An unsteady velocity field can then be reconstructed using only these modes and which therefore contains the flow field structures responsible for absorption of acoustic energy. The method is validated for both nonlinear and linear absorption regimes by comparing the energy of the reconstructed velocity field with the energy absorbed from the acoustic field. The good agreement obtained indicates the success of the technique presented. At the current time it is typically assumed the flow through an orifice is ideal except that fluid viscosity results in the generation of vorticity around the rim of the aperture. However, the improved understanding of the mechanisms by which energy is transferred out of the acoustic field, and into the unsteady velocity field, explains many of the observed absorption characteristics. This improved understanding should lead to the design of optimized damping systems. The presented methodology is also thought to be the basis by which numerical, CFD based, predictions relating to the absorption of acoustic waves should be analyzed and validated.

Written by J. Carrotte: j.f.carrotte@lboro.ac.uk, Loughborough University, UK.

5.4. Simultaneous multiplane PIV and microphone array measurements on a rod-airfoil configuration

The aeroacoustic sound generation process on a rod-airfoil configuration has been investigated by means of simultaneous particle-image-velocimetry (PIV) in the near-field and phased-microphone-array measurements in the far field. Up to 20 000 PIV snapshots per field of view have been recorded. Both measurements were conducted in a synchronized manner so as to enable the calculation of the cross-correlation of $R_{\Phi' p'}(\tau,\mathbf{x})$ between the acoustic pressure p' and a flow quantity Φ' at the points $\mathbf{x}$ derived from the measured velocity fluctuations (τ is the retarded time). The main idea of this concept was to use the coefficient matrix obtained from the aforementioned correlation to identify regularities in the near-field fluctuations that are related to the radiated far-field sound [23]. Fig. 12(a) shows the instantaneous distribution of the cross-correlation coefficients $R_{u'p'}$ and $R_{v'p'}$ for $\tau = 0$ depicted as a vector plot in the region near the airfoil leading edge. Flow structures mainly describing the vortex-airfoil interaction, which are supposed to be the main sources of noise, are extracted by the described method. The temporal evolution of $R_{v'p'}(\tau)$ at x/c=0.95 and y/c=0 near the leading edge of the airfoil is shown in Fig. 12(b). By an analysis of the temporal evolution of $R_{v'p'}$ the source region can be attributed to the leading edge of the airfoil [24].

Written by A. Henning: arne.henning@dlr.de, L. Koop and K. Ehrenfried, DLR, Germany.

5.5. A new microphone array for aeroacoustic measurements in a cryogenic environment

Measurement techniques based on microphone-arrays are well-known and common practice on scaled models in wind tunnels with closed test section. Usually, full-scale Reynolds numbers are not achieved. To increase the Reynolds number measurements are performed in cryogenic and/or pressurized wind tunnels. At the DLR Institute of Aerodynamics and Flow Technology the microphone array measurement technique was further developed to perform measurements in a cryogenic wind tunnel at temperatures down to 100 K. In order to use a microphone array in a cryogenic environment, coming to grips with cold hardiness and ensuring long-term stability of the array fairing and the electronic devices, especially the microphones, are the primary challenge. In a first step measurements of the radiated noise from a single rod configuration have been conducted in the cryogenic wind tunnel DNW-KKK using a prototype microphone array designed for cryogenic environment. Measurements were carried out with a wide range of operational flow parameters [25]. The measured sound radiation results showed a very good agreement with theory and a Reynolds number dependency of the measured and predicted sound power was shown. Based on these results, a microphone array for the application to airframe noise measurements has been developed and measurements have been performed in the same wind tunnel for various Reynolds numbers using a 9.24 percent Dornier-728 half model [26]. Fig. 13 shows a comparison of the source

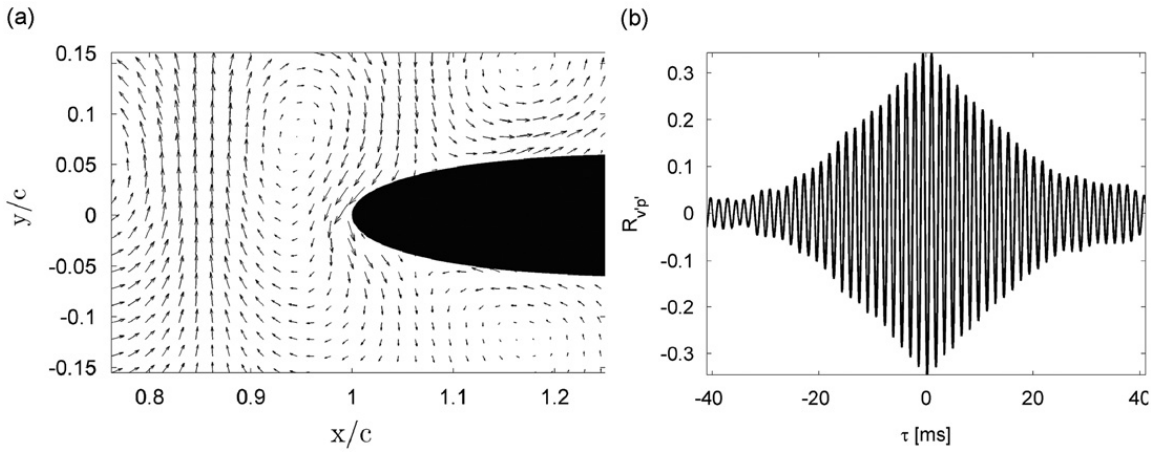

Fig. 12. Space–time cross-correlation coefficients $R_{u'p'}$ and $R_{v'p'}$ near the airfoil leading edge. The axes are scaled to the chord length c=0.15 m. (a) Space correlation ($\tau = 0$), (b) time correlation at x/c=0.95 and y/c=0.

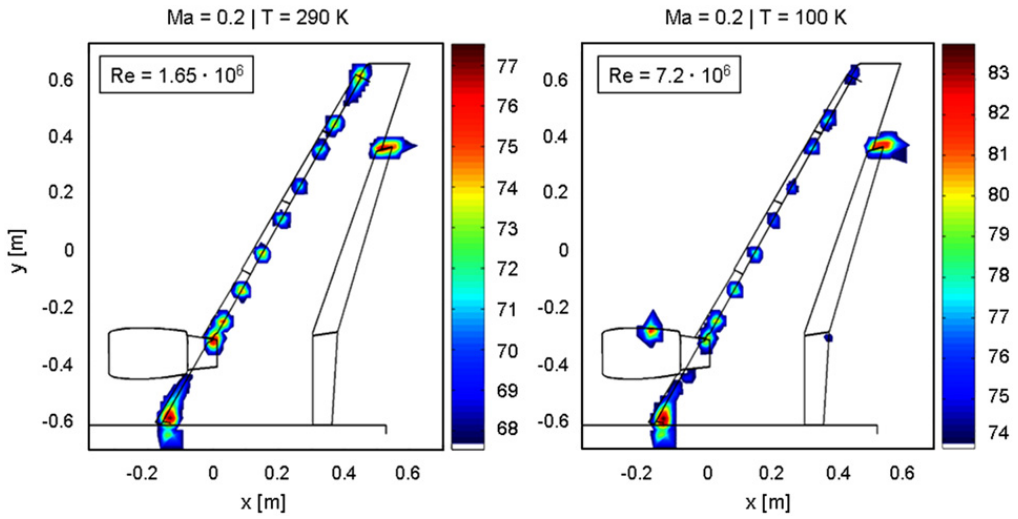

Fig. 13. Source maps of the DO-728 scale model at a Mach number of 0.2 but different Reynolds numbers and an angle of attack of 3°. The corresponding third-octave Strouhal number for both plots is St=90. The left plot shows the map at a temperature of 290 K which results in a Reynolds number of 1.65×10^6, whereas in the right plot a temperature of 100 K leads to an increased Reynolds number of 7.2×10^6.

maps for two different Reynolds numbers but the same Mach number and an angle of attack of 3°. Various sources in the slat region and on the flap-tip can be clearly identified in both cases. It can be seen that at the increased Reynolds number the general level is increased by about 6 dB. Remarkably, at the increased Reynolds number also a source at the nacelle strake can be seen. To our knowledge, this is the first time that airframe noise data have been acquired under these extreme cryogenic conditions.

Written by T. Ahlefeldt: thomas.ahlefeldt@dlr.de and L. Koop, DLR, Germany.

5.6. Optimization of the generalized inverse beamforming technique for aeroacoustic source quantification

Microphone array techniques, particularly beamforming methods, are commonly used for acoustic source localization and power estimation. The complex character of aeroacoustic applications, i.e. the distributed coherent source region with a variety of monopole, dipole and quadrupole noise contributions, imposes large challenges to conventional beamforming techniques and results in a decrease of the localization accuracy of this methodology. To overcome these problems, robust localization techniques, based on the microphone array cross-spectral eigenstructure, are emerging for aeroacoustic applications. One of these techniques, the generalized inverse beamforming method, has been thoroughly studied by the K.U. Leuven aeroacoustics research group with respect to the ability to model complex source regions, representative for aeroacoustic applications [27]. From this analysis, it is shown (Fig. 14) that the generalized inverse beamforming method largely improves the localization accuracy in comparison to conventional methodologies. However, it was noticed that the generalized inverse beamforming fails yielding accurate sound power estimations. Several approaches, including power estimations based on the cross-spectral matrix eigenvalues and analytical formulations, were adopted to overcome this drawback. As a result, an optimized regularization strategy is introduced, which defines a clear strategy to calculate the sound power estimation with improved accuracy. As an alternative, a new hybrid approach is proposed, which combines the localization accuracy of the generalized inverse beamforming technique with the accurate sound power estimation of the conventional beamforming methodology. In ongoing and future research, these experimental methodologies are combined with numerical prediction techniques for the aerodynamically generated noise sources and their in-duct propagation and far-field radiation to be able to quantify in-duct sound sources with microphone array measurements of the radiated acoustic far field.

Written by W. De Roeck: wim.deroeck@mech.kuleuven.be, P. A. G. Zavala and W. Desmet, Katholieke Universiteit Leuven, Belgium.

5.7. A weak scattering model for tone haystacking

Turbine-tone spectral broadening is caused by the interaction of the turbine tones radiated from the engine exhaust duct with the turbulence in the jet shear layer. The resulting scattered broadband field, known colloquially as a "haystack", can be measured well above the jet-noise broadband at some engine conditions. A weak scattering model for tone haystacking has been developed, based upon a model derived by A. Cargill in an internal Rolls-Royce report. The model can predict the far-field spectral density at different polar angles for tones radiated through a circular jet. An approximate form of Lilley's equation is used to model the scattering. The source terms in the scattering equation model acoustic/turbulent

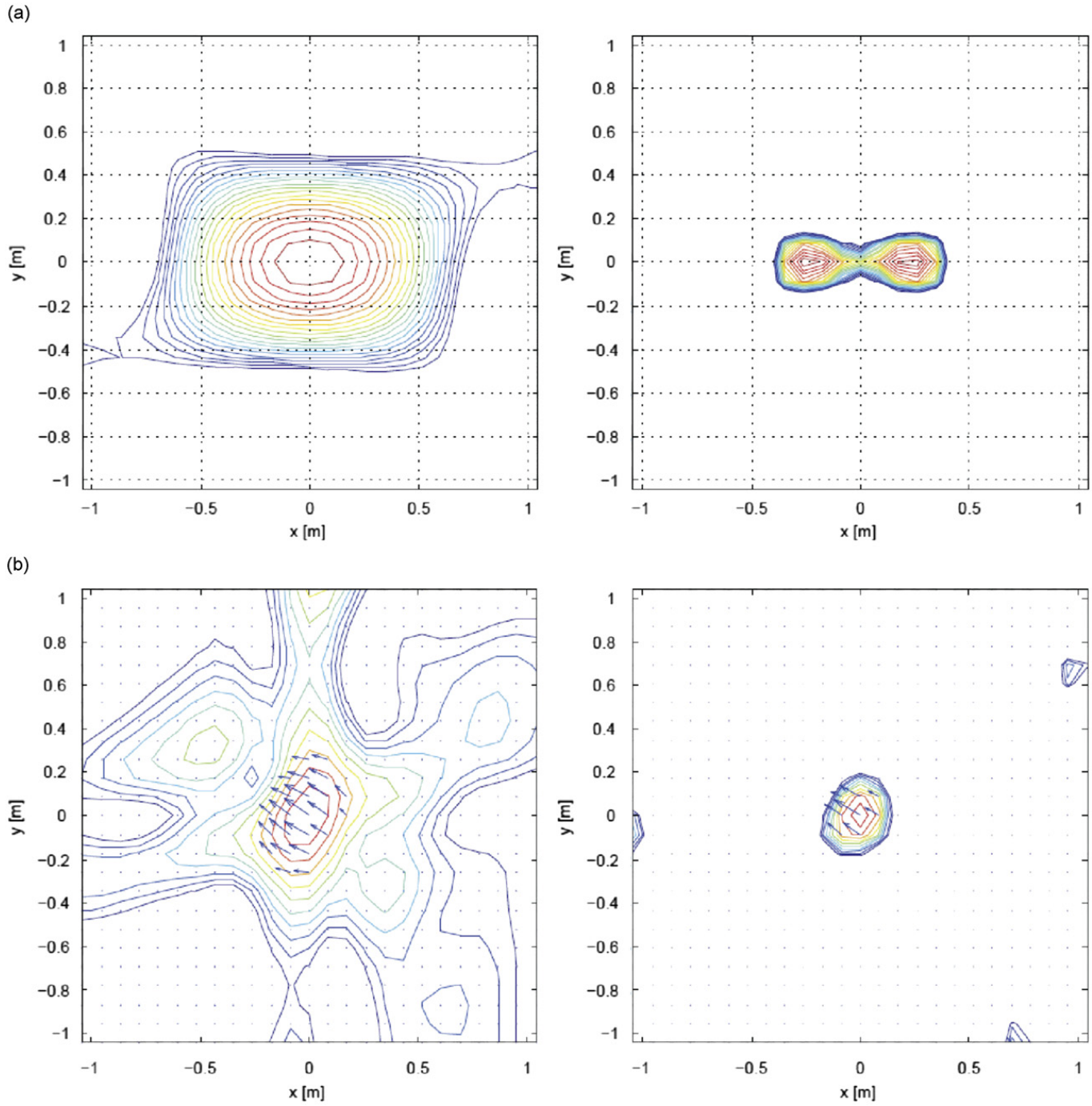

Fig. 14. Experimental determination of monopole and dipole sources (left: conventional, right: generalized inverse beamforming. Contour lines are in 10 dB range with 0.5 dB increment. (a) Two monopoles in-phase, (b) One dipole at 135 deg.

interactions. A weak-scattering approximation is used: it is assumed that the amplitude of the scattered field will be small compared to the incident field, so the acoustic field in the source terms can be approximated by the incident field. This enables the scattering equation to be solved using transform methods and high-frequency asymptotics. The result is an analytical model which gives relationships between the turbulence properties and the scattered field, for a circular jet. The solution can be used to predict the far-field spectral density at any polar angle, including inside the cone of silence, see McAlpine et al. [28]. Also, an approximate far-field solution valid at polar angles outside the cone of silence has been derived. This is closely related to the solution by Cargill which is also valid outside the cone of silence. Some typical examples of simulated ''haystacks'' are shown in Fig. 15 (reproduced from Ref. [28]). This shows the normalized far-field spectral density at polar angle equal to 90° of a tonal sound field which has undergone spectral broadening. The work was funded by the European sixth framework project TURNEX.

Written by A. McAlpine: am@isvr.soton.ac.uk, University of Southampton, UK.

5.8. Application of time domain impedance models for combustion noise prediction

The development of time domain impedance models to describe partial reflective boundaries has experienced a boost over the last four years. The newly developed and implemented impedance models enter into various applications now. One application of high importance is found in the field of combustion noise and combustion instabilities, which are both driven by the interaction of the flame with the acoustic reflections and the modes of vibration in the combustion chamber. Two examples of this application are given in Refs. [29,30]. In both cases, the extended Helmholtz resonator model is used to replace a resolved simulation of the settling chamber and inflow nozzle by an impedance boundary condition. By applying a time domain impedance boundary condition based on the extended Helmholtz resonator model, the swirl nozzle which would require an extremely complex meshing for a highly resolved 3D simulation, was reduced to an axi-symmetric problem. This significantly reduces the computational effort. Based on this, the excellent prediction of the transfer properties of the swirl combustion chamber shown in Fig. 16 was obtained by using an averaged LES result from Bender et al. [31] for the combustion and flow in the chamber, which did not show the correct acoustic properties, as base flow in a CAA simulation with the LEE. The model also replaces a settling chamber in the simulation of a model experiment for the generation of indirect combustion noise. In both cases the flow enters the domain normal to the surface. The boundary condition of Myers is not applicable as it can only account for the effect of a boundary layer parallel to the

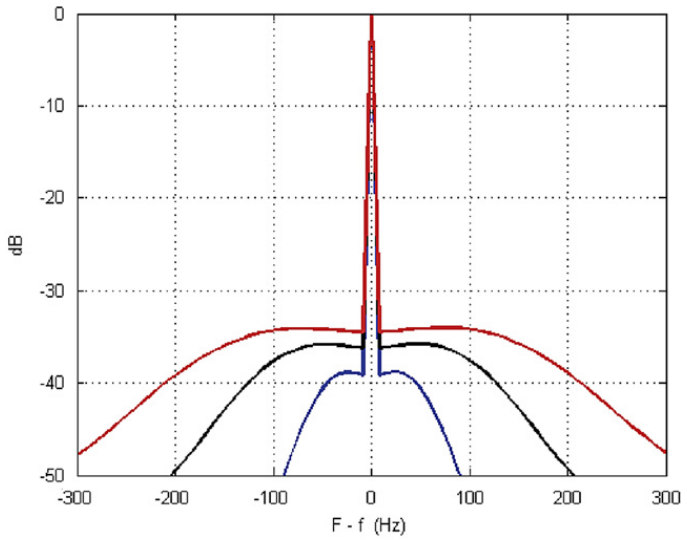

Fig. 15. Example of simulated tone haystacking (reproduced from Ref. [28]). The normalized far-field spectral density at polar angle equal to 90° is shown. The incident tone has frequency f Hz. Simulations have been conducted for three different jet velocities: the broadest spectrum is for the highest jet velocity, while the narrowest one is for the lowest jet velocity which were examined.

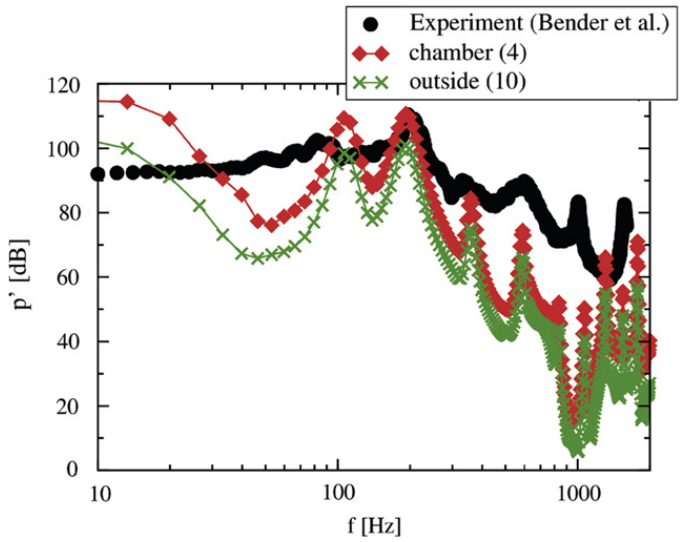

Fig. 16. Comparison between prediction (LES-LEE) and experimental results of the noise spectrum of a combustion chamber.

impedance surface. This also implies the absence of the Kelvin–Helmholtz instability in the simulations, which is linked to the Myers boundary condition.

Written by C. Richter: Christoph.Richter@TU-Berlin.de, Technische Universität Berlin, Germany.

5.9. Intensity based source identification and quality assessment for CAA

The acceptance and utilization of numerical methods is always linked to their reliably in practice. For CAA the prove is often limited to a general validation of the method at synthetic test cases featuring simplified flow conditions and geometries. This implies the risk of emerging spurious numerical errors for real problems, which could not be identified in advance. An acoustic intensity based method allows to assess the solution quality of each individual CAA result [32] and fills this gap. It is applied to quantify the dissipation error found in a numerical solutions for the propagation of tones, which are scattered into higher radial modes on their way through the axi-symmetric inlet of a centrifugal compressor. To remain with a structured mesh, a Chimera technique is applied. The sound field is shown in the upper part of Fig. 17. The intensity analysis is shown below. It verifies the dissipation error remains below 3 percent and assures the correctness of the following radial mode analysis. Furthermore, the acoustic intensity allows an identification of the radiating acoustic sources or sources of numerical error in the simulation. The average source strength equals the divergence of the acoustic intensity in average. The method has been applied for the identification of sources of indirect combustion noise from a simulation of a model experiment as shown in Fig. 18 [33,30]. Both methods are, however, not limited to aeroacoustic propagation problems. Rather they have the potential to assess the propagation properties and identify acoustic sources for unsteady fluid dynamic simulations in general. This may extend the standard toolbox of post processing and analysis methods for CAA and CFD simulations. However, a decomposition of the velocity field into vorticity and acoustic modes is required for general application.

Written by C. Richter: Christoph.Richter@TU-Berlin.de, Technische Universitt Berlin, Germany.

5.10. High performance higher-order BEM and boundary-to-far-field aeroacoustic transfer function

In Refs. [34,35], new boundary elements and finite elements based on the Coons patch concept for the description of the dependent and independent variables have been developed and assessed, as well as innovative technique for the fast evaluation of the BEM matrices, based on the exploitation of the SIMD vector extensions present in the modern computer

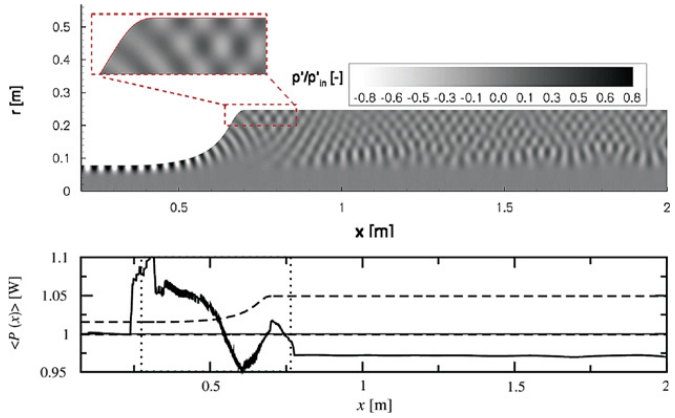

Fig. 17. Instantaneous pressure contours (top) and acoustic energy conservation (below) in the opening inlet duct of a centrifugal compressor.

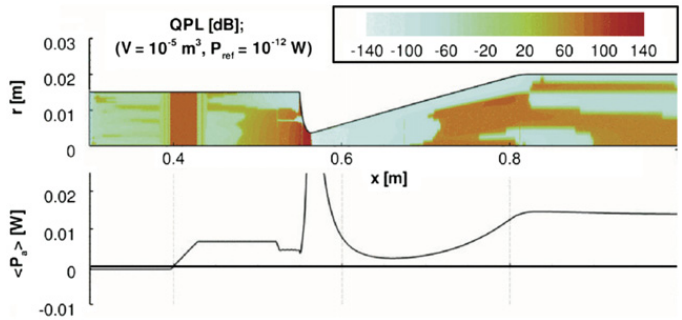

Fig. 18. Identification of radiating acoustic sources, shown as source power level [32] (top) and acoustic energy flux (below) for a transonic nozzle in response to an electrical heating pulse.

architectures. In parallel, a power-spectral-density transfer function for the evaluation of the aeroacoustic field has been developed by coupling a potential-vorticity decomposition of the velocity field with a boundary integral formulation for the velocity potential [36]. Preliminary assessment reveals an excellent agreement with available experimental data. Dedicated experimental campaigns are planned in the near future to fully assess the formulation.

Written by U. Iemma: u.iemma@uniroma3.it, L. Morino, G. Caputi-Gennaro and R. Camussi, University Roma Tre, Italy.

5.11. A turbomachinery tone noise 3D analysis method based on a linearized approach with 3D non-reflecting conditions

A time-linearized 3D aeroacoustic solver for turbomachinery applications, named Lars, was equipped with three-dimensional non-reflecting boundary conditions at the University of Florence [37]. This solver had been previously developed for aeroelastic flutter analysis, and then extended to aeroacoustic tone noise simulations, in the context of a long-term collaboration between University of Florence and Avio Group. The Lars solver is specifically designed to work together with the Traf steady/unsteady aerodynamic solver [38]. Three-dimensional non-reflecting boundary conditions are based on duct wave propagation theory. The problem of determining the shape of the waves (radial modes) that may be present in a cylindrical or annular duct with a given possibly swirling and/or sheared mean flow cannot be solved analytically in the general case: it is solved numerically by discretizing the Euler equations on a radial one-dimensional grid; radial modes are searched for as solutions for a complex generalized eigenvalue problem, and are classified into acoustic modes and nearly-convected ones [39]. By decomposing perturbations in radial modes, non-reflecting boundary conditions are able to allow outgoing perturbations to pass, while suppressing or assigning incoming ones. A number of validation tests were performed, among which the 3rd CAA Workshop Cat. 4 benchmark problem (Fig. 19), showing good agreement with other methods.

Written by F. Poli: Francesco.Poli@arnone.de.unifi.it, University of Florence, Italy.

5.12. A hybrid method for CAA

For the simulation of aeroacoustic phenomena around complex structures the application of unstructured grids is advantageous close to the geometry to enable a fast mesh generation. In the far-field structured grids are preferable to save computational effort. The objective of this project is to couple schemes that work on those different grid types. Two sophisticated solvers for the linearized acoustic equations were chosen for this work: the computation on the structured grid is done by PIANO (provided by the Institute of Aerodynamics and Flow Technology (IAS) at the German Aerospace Center (DLR) in Braunschweig). It applies a DRP finite difference scheme of 4th order for the discretization in space and Runge–Kutta schemes of 4th or 6th order in time. For the unstructured grid the high order discontinuous Galerkin solver NoisSol (developed by the Institute of Aerodynamics and Gasdynamics at Universität Stuttgart) is applied. The decomposition of the computational domain is done with nonoverlapping grids with straight coupling interfaces. MPI is used to exchange the information between the coupling partners, which is then included using ghost cells or ghost points, respectively. Since this project is aimed at an user friendly framework for industrial application, the automation of the

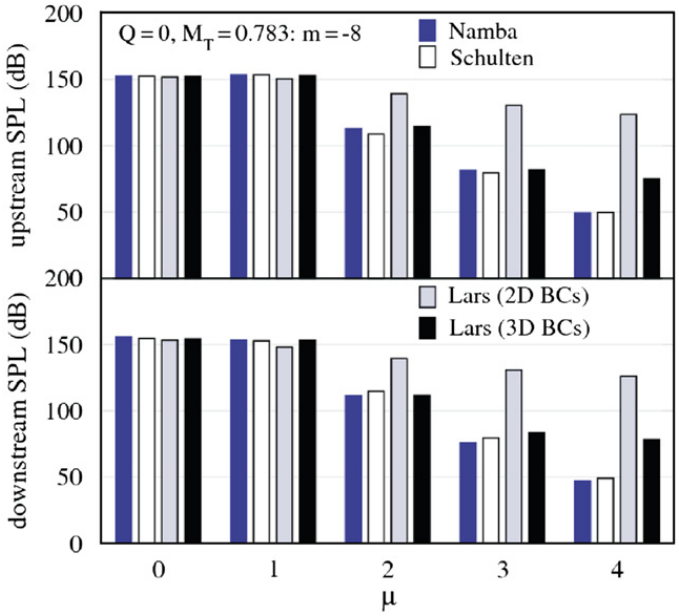

Fig. 19. Some 3rd CAA Workshop Cat. 4 benchmark problem results compared to numerical results with 2D boundary conditions and to lifting surface theory results.

preprocessing and initialization is an important issue. The calculation results showed the operability of the coupling and its ability to maintain the order of accuracy of the single solvers.

Written by A. Birkefeld: Andreas.Birkefeld@iag.uni-stuttgart.de and C.-D. Munz, Universitt Stuttgart, Germany.

6. Rotorcraft noise

6.1. 3D sound directivity around a helicopter turboshaft engine

It is known that turboshaft engines can be the main source of noise due to a helicopter at take-off. Some new silencing devices of the inlets and of the ejector were designed for a Turbomeca Arrius 2B2 engine in the framework of the European project Friendcopter [40] were tested in the Turbomeca open-air static facility. Intake and exhaust are not axi-symmetric, and conventional directivity patterns of the sound field on a horizontal arc of circle are insufficient. A special microphone array was assembled on a vertical semicircular strut perpendicular to the engine centerline and translating axially, as pictured in Fig. 20(a). Data processing has been implemented to plot maps of sound pressure levels in third-octave bands and to compute the sound power levels. Intake and exhaust radiations were separated thanks to mufflers on the other side. The lined fins in the secondary lateral inlet well reduce the compressor tone which is largely dominant in intake radiation, as illustrated in Fig. 20(b). Its sound power level is decreased by 7 dB. The Friendcopter ejector also is successful to reduce exhaust broadband noise above 1 kHz with a gain of 5 dB on sound power level, as shown in Fig. 20(c). Flight tests on a EC135 helicopter have shown how the gains on engine noise affect the aircraft sound level.

Written by H. Gounet and S. Lewy: Serge.Lewy@onera.fr, ONERA, France.

7. Propeller noise

7.1. Aeroacoustic optimization of a pusher propeller

CIRA has improved an existing multidisciplinary analysis methodology for the evaluation of aerodynamic performances and acoustic impacts of aircraft propellers [41] by including in the simulation code network new modules for the prediction of the broadband component of noise. The updated analysis block has been embedded into an optimization environment to study the influence of the exhaust on the acoustic signature of a pusher propeller configuration [42]. The study has covered both the tonal and broadband noise calculation. The tonal noise results from the periodic flow unsteadiness due to the non-axial flight and to the impingement of the engine exhausts on the propeller disk. The broadband noise is mainly due to the interaction between the blade leading-edge and the exhaust turbulence. Although broadband noise contributions for rotors and propellers are generally nonnegligible, the present investigations have shown that the tonal noise contribution, due to the high-speed flow in the tip region and the blade-exhaust interaction in the inner part of the blade, plays a dominant role (Fig. 21). The optimization has affected the exhaust radial position in the propeller disk and the aerodynamic shape of the blade under the direct influence of the exhaust. The optimization has revealed that the overall acoustic energy of the pusher propeller can be reduced up to a value of 3.5 dB.

Written by A. Pagano: a.pagano@cira.it, M. Barbarino, D. Casalino and L. Federico, CIRA, Italy.

7.2. Aerodynamic and aeroacoustic analysis of installed pusher propeller aircraft configurations

The aeroacoustic phenomena characteristic of a pusher-propeller configuration and their aerodynamic causes are discussed and analyzed. The work was done in the frame of the European-funded project CESAR (Cost Effective Small

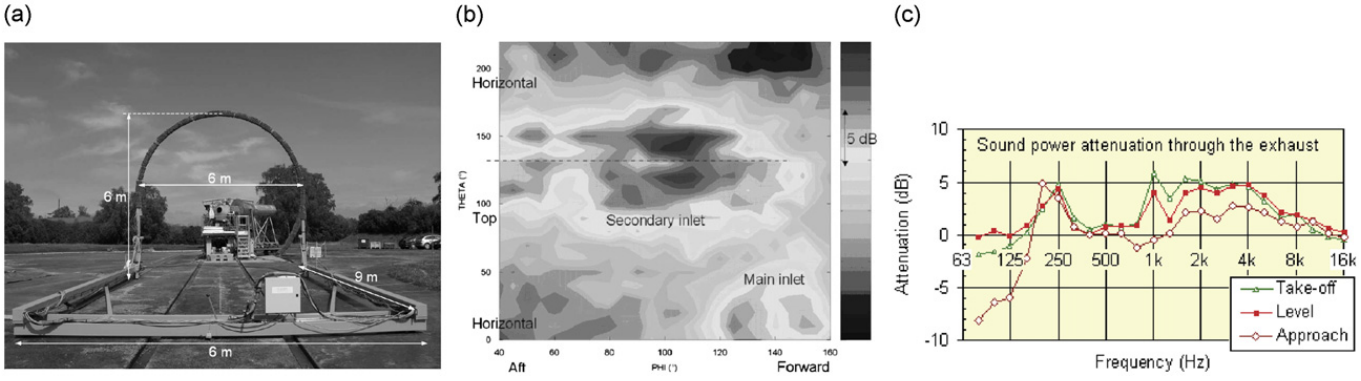

Fig. 20. Arrius 2B2 turboshaft sound directivity measurements. (a) Acoustic array downstream engine mounted on the test platform, (b) intake radiation at the compressor blade passing frequency: secondary plenum with rigid fins, take-off, third octave 10 kHz, (c) attenuation of the sound pressure calculated on the upper half-sphere due to the Friendcopter ejector.

AiRcraft). The configuration under study is an industrially relevant design with a wing-mounted pusher propeller, which features a close coupling of the turboshaft engines exhaust nozzles and a five bladed propeller. An established numerical analysis approach is applied in this study, which couples a high-fidelity unsteady aerodynamic simulation using the DLR TAU-Code with the DLR FW-H code APSIM for a subsequent aeroacoustic evaluation. A detailed analysis of the contributions of various components of the installation, as well as flight condition specific parameters toward the overall noise generation by the propeller is presented in Ref. [43]. The CFD results revealed strong mutual interactions between the propeller and the engine jet, leading to strong periodic fluctuation of the blade loads. The interaction of the engine jets and the blade wakes and tip vortices is clearly visible in Fig. 22(a). Ground noise directivities as A-weighted SPL for various configurations are shown in Fig. 22(b). The configuration that includes the engine jet simulation (marked as "Engine On"), indicates that the contribution of the propeller-jet interaction leads to an increase in maximum noise of about 6.5 dB when compared with the same configuration with the engine simulation turned off (marked as "Engine Off"). Comparing this latter case with the isolated propeller at axial flow (marked as "Isolated"), it can be seen that the combined effect of the installation of the propeller on the aircraft—primarily the effect of the wing wakes—as well as the angle of attack increases maximum noise emissions by about 6 dB.

Written by J. Yin: jianping.yin@dlr.de and A. Stuermer, DLR, Germany, and M. Aversano, Piaggio, Italy.

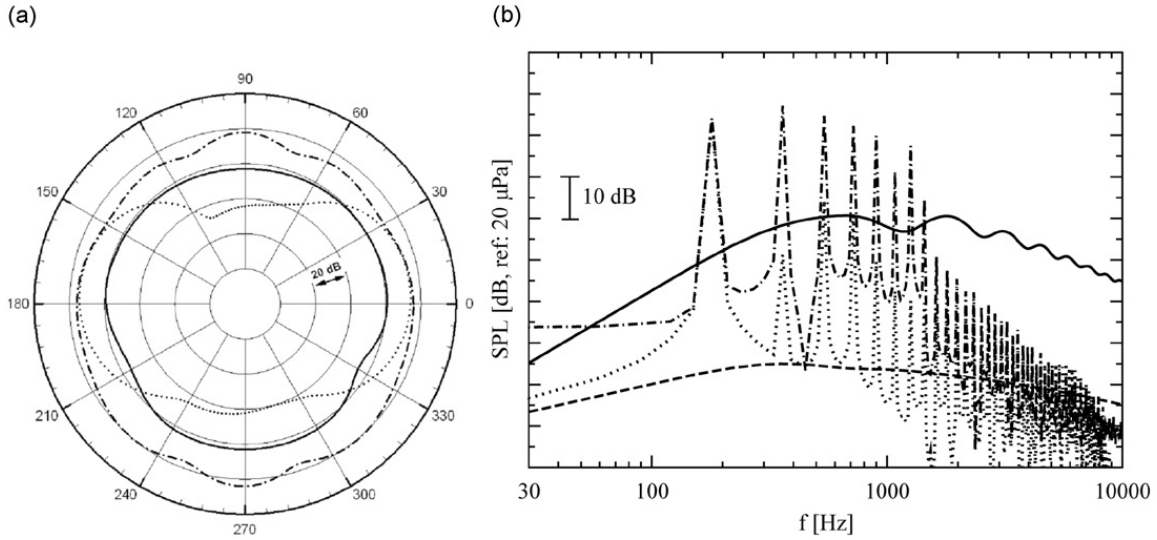

Fig. 21. Computed propeller noise directivity patterns and SPL spectra. Comparison between: tonal noise (dashed-dotted line), tonal noise with no exhaust (dotted line), overall broadband noise (solid line), and trailing edge noise (dashed line). (a) Overall SPL directivity, (b) SPL at 45° away from the propeller axis.

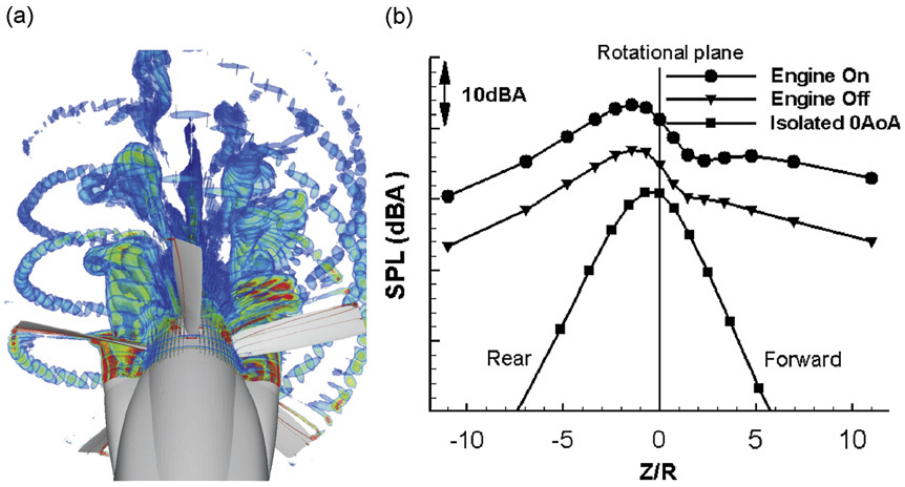

Fig. 22. Computation of installed pusher propeller aircraft noise. (a) Vorticity contours showing engine jet-propeller interactions, (b) ground noise directivities as A-weighted SPL for various configurations.

7.3. Low-speed aerodynamics and aeroacoustics of CROR propulsion systems

Contra rotating open rotor (CROR) propulsion systems have come back into focus as a possible economic and environmentally friendly powerplant for future transport aircraft. Having been widely applied to the simulations of single rotation propellers, the DLR CFD code TAU and the aeroacoustic analysis tool APSIM have been employed for the analysis of the complex aerodynamics and aeroacoustics of this type of aircraft propulsion system [44]. In order to develop an understanding of the impact of configuration variations, a generic 8×8 and 10×8 pusher CROR powerplant are studied here at typical sea-level take-off conditions. The results allow for a detailed analysis of the aerodynamic interactions between the two rotors as well as the noise generation mechanisms, allowing for an improved understanding of interaction tone sources [45]. The simulations show that the increase in the blade number in the front rotor for the 10×8 configuration allows for an unloading of each blade versus the 8×8 CROR. This leads to reductions in the front blades wake deficit and tip vortex intensity, resulting in a notable decrease in the unsteady oscillation amplitudes in the aft rotors blade loadings. A nearfield aeroacoustic analysis shows that these decreases in unsteady loading translate into noise reductions of up to 6 dB in particular in the upstream and downstream radiation directions, as shown by the contour plot in Fig. 23(b). The noise emissions in the far field are seen to be dominated by the interaction tones for all observer locations and most strongly so in both the up- and downstream direction. Furthermore, a comparative analysis of the CROR noise emissions employing both the permeable as well as the impermeable FW-H formulations indicates that quadrupole noise sources play an important role even at low-speed flight conditions.

Written by A. Stuermer: arne.stuermer@dlr.de and J. Yin, DLR, Germany.

7.4. Coupled hydrodynamics–hydroacoustics BEM modelling of marine propellers

Important issues in the framework of marine propeller hydroacoustics are the evaluation of radiated noise and pressure fluctuations induced on the hull surface. The analysis of these problems requires that both the hydrodynamic interactions between hull and propeller and the effects of the hull surface-scattering are modeled. In particular, emission sources associated to the propeller are characterized by strong blade loading fluctuations due to the fact that the propeller operates in a non-homogeneous, turbulent hull-induced wakefield. Furthermore, when blade loading or speed are large, transient cavitation occurs with a relevant impact on propeller noise footprints. Focusing on the numerical prediction of hull-pressure pulses, a multidisciplinary approach is required to model accurately: (i) hydrodynamic sources of hydroacoustics loads impinging the hull, (ii) sound radiation from the propeller to the hull and (iii) the interaction between the moving hull and acoustics waves. The authors have addressed the problem in Ref. [46] through a coupled hydrodynamics–hydroacoustics BEM model. Specifically, the Ffowcs-Williams and Hawkings (FW–H) equation for porous surfaces has been applied to describe the effects of transient blade cavitation on noise emission and radiation in unbounded space. Propeller flow predictions are obtained through a BEM for potential flows combined with an unsteady sheet cavitation model. Acoustics results have been compared with those obtained by a standard approach based on the generalized Bernoulli equation. The presence of the hull-plate surface is introduced in a second step of the analysis in which pressure pulses on the hull-plate are obtained by solving the flow field around the propeller in the presence of the hull-plate. However for a realistic propeller-hull configuration, the above approach results to be very time-consuming. In order to overcome such a drawback, the scattering formulation proposed in Ref. [47] and based on the FW–H equation may be successfully applied. The mentioned scattering modelling has been applied for the prediction of the hull-pressure fluctuations on a realistic marine configuration.

Written by F. Salvatore, C. Testa and L. Greco, INSEAN - Italian Ship Model Basin, Italy.

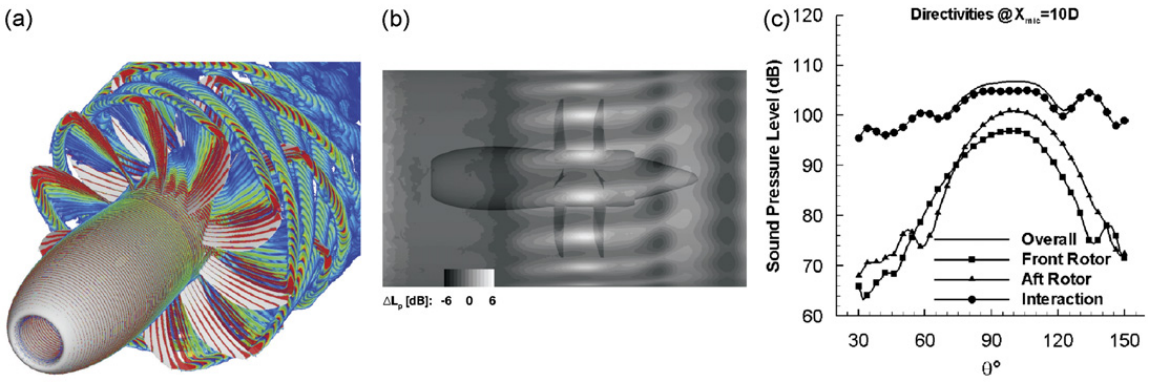

Fig. 23. Computation of CROR noise. (a) Wake and vortex system, (b) nearfield noise reductions due to increased blade count in front rotor, (c) 10×8 CROR far-field noise directivity decomposition.

8. Miscellaneous topics

8.1. Aeroacoustics of periodic pipe systems with multiple closed side-branches

Experiments [48] carried out on a scale model of a gas transport compressor station show that a system with six deep side branches displays strong trapped modes. The scale model reproduces the field behaviour and it has been used to test design rules aiming at a reduction of pulsation levels. The most commonly used solution, detuning of the side branch length, appears to be inefficient. Systems with up to 19 shallow side branches [49,50] produce flow-induced pulsations, triggered by the global longitudinal acoustic modes of the pipe system. This behaviour has been demonstrated to be similar to that of corrugated pipes. Moreover, our experiments and theoretical analysis demonstrate that the aeroacoustic sources are located near the acoustic pressure nodes of the longitudinal acoustic modes.

Written by D. Tonon: D. Tonon@tue.nl, G. Nakiboglu and A. Hirschberg, Eindhoven University of Technology, The Netherlands.

8.2. Multidisciplinary design optimization and aircraft noise reduction

The development of the optimization environment FRIDA (Framework for Innovative Design in Aeronutics) proceeds in the direction of an increasing reliability of the computing framework in presence of community noise requirements. Specifically, the algorithm has been enriched with the capability to handle uncertainties of various kinds, in order to improve the robustness of the optimal solution. In addition, the extension to multi-fidelity models has been completed, including the possibility to deal with a "cascade" of models of different accuracy. FRIDA is currently used within the FP7 Level-1 EC-funded project COSMA (Community Oriented Solutions to Minimize aircraft noise Annoyance) to optimize a complex airport scenario taking into account the forthcoming noise abatement technologies. The same optimization tool is going to be used within the FP7 Level-2 EC-funded project OPENAIR (OPtimisation for low Environmental Noise impact of AIRcraft). In that context, the analysis will be limited to the aeroacoustic assessment of a blended-wing-body configuration, and the need of a multidisciplinary approach stems from the unconventionality of the analyzed concept and the requirement of a careful check of the fulfillment of the aerodynamic and stability constraints under the action of the control surfaces.

Written by U. Iemma: u.iemma@uniroma3.it and M. Diez, University Roma Tre, Italy.

8.3. Cabin noise control in turboprop aircraft through smart actuators

The issue of interior noise alleviation on propeller-driven aircraft has been faced by the authors in Ref. [51]. In such a work, a conventional mid-range turboprop aircraft has been considered; to achieve the desired noise abatement, a control strategy based on the actuation of fuselage-embedded piezoelectric (PZT) patches has been applied. The control law has been obtained through an optimal harmonic LQR formulation considering a comprehensive aeroacoustoelastic model including interior acoustics, smart shell dynamics and fuselage scattering. Specifically, the numerical model considers the fuselage to be a smart thin cylindrical shell with PZT patches embedded; shell dynamics and cabin acoustics are solved jointly in the frequency-domain through the Galerkin method. To close the problem, a scattering model, able to accurately describe the interaction between the fuselage and the external impinging acoustic wave, is included. A classical LQR-optimal-control-synthesis criterion is applied to yield a suitable control law driving actuators. The guidelines deriving from this research indicate that PZT actuators are well suited for control noise purposes only when smart patches are placed at points where resonant acousto-structural modes have higher amplitudes. Furthermore, an unbalanced voltage distribution among PZTs might arise. These drawbacks suggest the use of an optimized control actuator placement and control weighting coefficients search. The enhancement of the prediction numerical tools used in Ref. [51] through a dedicated optimization tool represents the core of the on-going research activity on cabin noise.

Written by C. Testa: c.testa@insean.it, INSEAN - Italian Ship Model Basin, G. Bernardini and M. Gennaretti, University Roma Tre, Italy.

References

[1] R. Ewert, Broadband slat noise prediction based on caa and stochastic sound sources from a random particle-mesh (rpm) method, *Computers and Fluids* 37 (4) (2008) 369–387.
[2] D. König, S.R. Koh, M. Meinke, W. Schröder, Two-step simulation of slat noise, *Computers and Fluids* 39 (3) (2010) 512–524.
[3] S.R. Koh, W. Schröder, M. Meinke, Sound generation control by fluid bleeding, AIAA Paper 2009-3225.
[4] I. Cozza, R. Arina, A. Iob, Broadband trailing edge noise prediction with a stochastic source model, Euronoise 2009, Edinburg, Scotland, UK, 26–28 October 2009.
[5] T. Brooks, D. Pope, M. Marcolini, Airfoil self-noise and prediction, NASA Technical Report, Reference Publication 1218.
[6] S. Oerlemans, J.G. Schepers, Prediction of wind turbine noise and validation gainst experiment, *International Journal of Aeroacoustics* 8 (6) (2009) 555–584.
[7] C. Bogey, C. Bailly, An analysis of the correlations between the turbulent flow and the sound pressure fields of subsonic jets, *Journal of Fluid Mechanics* 583 (2007) 71–97.
[8] C. Bogey, S. Barré, D. Juvé, C. Bailly, Simulation of a hot coaxial jet: direct noise prediction and flow-acoustics correlations, *Physics of Fluids* 21 (2009) 1–14.

[9] S. Redonnet, C. Mincu, E. Manoha, Computational aeroacoustics of realistic coaxial engines, AIAA Paper 2008-2826.
[10] S. Redonnet, C. Mincu, E. Manoha, A. Sengissen, B. Caruelle, Computational aeroacoustics of a realistic coaxial engine in subsonic and supersonic take-off conditions, AIAA Paper 2009-3240.
[11] S. Redonnet, E. Manoha, P. Sagaut, Numerical simulation of propagation of small perturbations interacting with flows and solid bodies, AIAA Paper 2001-2223.
[12] S. Redonnet, Simulation de la propagation acoustique en présence d'écoulements quelconques et de structures solides, par résolution numérique des équations d'euler (simulation of acoustic propagation in the presence of generic flows and solid bodies through numerical solution of the euler equations), PhD Thesis, Université Bordeaux I, France, November 2001.
[13] A. Iob, R. Arina, C. Schipani, Numerical prediction method for turbomachinery noise radiation through the engine exhaust, AIAA Paper 2009-3287.
[14] A. Iob, R. Arina, C. Schipani, A frequency-domain linearized euler model for turbomachinery noise radiation through engine exhaust, *AIAA Journal* 48 (4) (2010) 848–858.
[15] P.R. Amestoy, I.S. Duff, J.Y.L. Excellent, Multifrontal parallel distributed symmetric and unsymmetric solvers, *Computational Methods in Applied Mechanical Engineering* 184 (2000) 501–520.
[16] E.J. Brambley, Fundamental problems with the model of uniform flow over acoustic linings, *Journal of Sound and Vibration* 322 (4–5) (2009) 1026–1037.
[17] Y. Aurégan, M. Leroux, Experimental evidence of an instability along an impedance wall with flow, *Journal of Sound and Vibration* 317 (3–5) (2008) 432–439.
[18] D. Marx, Y. Aurégan, H. Bailliet, J.C. Valière, Experimental evidence of hydrodynamic instability over a liner in a duct with flow, AIAA paper 2009-3170.
[19] M. Taktak, J.M. Ville, M. Haddar, G. Gabard, F. Foucart, Acoustic liners behavior investigation using the multimodal scattering matrix, *International Review of Mechanical Engineering* 2(4).
[20] A. Sitel, J.M. Ville, F. Foucart, Multiload experimental procedure for measurement of acoustic scattering matrix of a duct discontinuity for higher order modes propagation conditions, *Journal of Acoustical Society of America* 120 (5) (2006) 2478–2490.
[21] G. Berkooz, P. Holmes, J.L. Lumley, The proper orthogonal decomposition in the analysis of turbulent flows, *Annual Review of Fluid Mechanics* 25 (1993) 539–575.
[22] J. Rupp, J.F. Carrotte, A. Spencer, Interaction between the acoustic pressure fluctuations and the unsteady flow field through circular holes, *Journal of Engineering for Gas Turbines and Power GT2009-59263 GTP-09-1090* 132 (6) (2010) 061501-1–061501-9.
[23] A. Henning, K. Kaepernick, K. Ehrenfried, L. Koop, A. Dillmann, Investigation of aeroacoustic noise generation by simultaneous particle image velocimetry and microphone measurement, *Experiments in Fluids* 348 (2008) 1073–1085.
[24] A. Henning, L. Koop, K. Ehrenfried, A. Lauterbach, S. Kroeber, Simultaneous multiplane piv and microphone array measurements on a rod-airfoil configuration, AIAA Paper 2009-3184.
[25] T. Ahlefeldt, L. Koop, Microphone array measurement in a cryogenic wind tunnel, AIAA Paper 2009-3185.
[26] T. Ahlefeldt, A. Lauterbach, L. Koop, Aeroacoustic high reynolds number measurements of a scaled half model, AIAA Paper 2010-3748.
[27] P.A.G. Zavala, W.D. Roeck, J.R.F. Arruda, W. Desmet, Monopole and dipole identification using generalized inverse beamforming, AIAA Paper 2010-3740.
[28] A. McAlpine, C.J. Powles, B.J. Tester, A weak scattering model for tone haystacking, AIAA Paper 2009-3216.
[29] C. Richter, L. Panek, V. Krause, F. Thiele, Investigations regarding the simulation of wall noise interaction and noise propagation in swirled combustion chamber flows, in: A. Schwarz, J. Janicka (Eds.), *Combustion Noise*, DFG Research Unit 486, Springer, 2009, pp. 217–238.
[30] C. Richter, D. Morgenweck, F. Thiele, Caa simulation and intensity based evaluation of a model experiment for indirect combustion noise, *Acta Acoustica United with Acoustica* 95 (3) (2009) 479–492.
[31] C. Bender, F. Zhang, P. Habisreuther, H. Büchner, H. Bockhorn, *Combustion Noise, Chapter 2: Measurement and Simulation of Combustion Noise emitted from Swirl Burners*, Springer, Berlin, Heidelberg, pp. 33–62.
[32] C. Richter, K. Ehrenfried, N. Schönwald, M. Steger, F. Thiele, Acoustic intensity based data analysis and assessment in computational aeroacoustics, *Journal of Sound and Vibration* 327 (3–5) (2009) 490–506.
[33] F. Bake, C.R.C.B. Mühlbauer, N. Kings, I. Röhle, F. Thiele, B. Noll, The entropy wave generator: a reference case on entropy noise, *Journal of Sound and Vibration* 326 (3–5) (2009) 574–598.
[34] U.Iemma, L. Morino, R. Camussi, G. Caputi-Gennaro, On the sound generated by boundary-layer vorticity, *Acoustics'08*, 2009.
[35] U. Iemma, On the use of a simd vector extension for the fast evaluation of boundary element method coefficients, *Advances in Engineering Software* 41 (2010) 451–463.
[36] L. Morino, G. Caputi-Gennaro, R. Camussi, U. Iemma, Power-spectral-density boundary-to-field transfer function, AIAA Paper 2008-3002.
[37] F. Poli, A. Arnone, C. Schipani, A 3D linearized method for turbomachinery tone noise analysis with 3D non-reflecting boundary conditions, *8th European Conference on Turbomachinery Fluid Dynamics and Thermodynamics (ETC)*, Graz, Austria, 2009.
[38] A. Arnone, Viscous analysis of three-dimensional rotor flow using a multigrid method, *Journal of Turbomachinery* 116 (1994) 435–445.
[39] M. Montgomery, J. Verdon, A three-dimensional linearized unsteady euler analysis for turbomachinery blade rows, NASA Contractor Report 4770.
[40] P.L. Regaud, E. Bouty, A. Vallon, D. Derbez, P. Baude, Liner integration on a turboshaft engine: successful example of performance trade-off, AIAA Paper 2009-3328.
[41] A. Pagano, L. Federico, M. Barbarino, F. Guida, M. Aversano, Multi-objective aeroacoustic optimization of an aircraft propeller, AIAA Paper 2008-6059.
[42] A. Pagano, M. Barbarino, D. Casalino, L. Federico, Tonal and broadband noise calculations for aeroacoustic optimization of propeller blades in a pusher configuration, AIAA Paper 2009-3138.
[43] J. Yin, A. Stuermer, M. Aversano, Coupled urans and fw-h analysis of installed pusher propeller aircraft configurations, AIAA Paper 2009-3332.
[44] A. Stuermer, Unsteady cfd simulations of contra-rotating propeller propulsion systems, AIAA paper 2008-5218.
[45] A. Stuermer, J. Yin, Low-speed aerodynamic and aeroacoustic analysis of cror propulsion systems, AIAA Paper 2009-3134.
[46] F. Salvatore, C. Testa, L. Greco, Coupled hydrodynamics-hydroacoustics bem modelling of marine propellers operating in a wakefield, *Smp09, First International on Marine Propulsors*, Trondheim, Norway, 2009.
[47] M. Gennaretti, C. Testa, Prediction of sound scattering by elastic moving bodies, *Journal of Sound and Vibration* 314 (3–5) (2008) 712–737.
[48] D. Tonon, G. Nakiboglu, J.F.H. Willems, A. Hirschberg, R.E. Leandro, W. Polifke, H.J. Riezebos, Self-sustained aeroacoustic oscillations in multiple side branch pipe systems, AIAA Paper 2009-3262.
[49] D. Tonon, B.J.T. Landry, S.P.C. Belfroid, J.F.H. Willems, G.C.J. Hofmans, A. Hirschberg, Whistling of a pipe system with multiple side branches: comparison with corrugated pipes, *Journal of Sound and Vibration* 329 (8) (2009) 1007–1024.
[50] G. Nakiboglu, S.P.C. Belfroid, D. Tonon, J.F.H. Willems, A. Hirschberg, A parametric study on the whistling of multiple side branch system as a model for corrugated pipes, *ASME Pressure Vessels and Piping Division Conference*, Prague, Czech Republic, 2009.
[51] C. Testa, G. Bernardini, M. Gennaretti, Cabin noise alleviation through fuselage skin embedded smart actuators, AIAA Paper 2009-3243.